Neurobiology of Aging 124 (2023) 71–84

Contents lists available at ScienceDirect

Neurobiology of Aging

journal homepage: www.elsevier.com/locate/neuaging.org

Regular Article

Orexin-A aggravates cognitive deficits in 3xTg-AD mice by exacerbating synaptic plasticity impairment and affecting amyloid β metabolism

Yi-Ying Li[a], Kai-Yue Yu[a], Yu-Jia Cui[a], Zhao-Jun Wang[a], Hong-Yan Cai[a,b], Ji-Min Cao[a,*], Mei-Na Wu[a,*]

[a] Department of Physiology, Key Laboratory of Cellular Physiology, Ministry of Education; Key Laboratory of Cellular Physiology in Shanxi Province, Shanxi Medical University, Taiyuan, Shanxi, China
[b] Department of Microbiology and Immunology, Shanxi Medical University, Taiyuan, Shanxi, China

ARTICLE INFO

Article history:
Received 30 June 2022
Revised 9 January 2023
Accepted 13 January 2023
Available online 18 January 2023

Keywords:
Alzheimer's disease
Orexin-A
Cognition
Long-term potentiation
β-amyloid protein
Tau phosphorylation

ABSTRACT

Dementia is the main clinical feature of Alzheimer's disease (AD). Orexin has recently been linked to AD pathogenesis, and exogenous orexin-A (OXA) aggravates spatial memory impairment in APP/PS1 mice. However, the effects of OXA on other types of cognitive deficits, especially in 3xTg-AD mice exhibiting both plaque and tangle pathologies, have not been reported. Furthermore, the potential electrophysiological mechanism by which OXA affects cognitive deficits and the molecular mechanism by which OXA increases amyloid β (Aβ) levels are unknown. In the present study, the effects of OXA on cognitive functions, synaptic plasticity, Aβ levels, tau hyperphosphorylation, BACE1 and NEP expression, and circadian locomotor rhythm were evaluated. The results showed that OXA aggravated memory impairments and circadian rhythm disturbance, exacerbated hippocampal LTP depression, and increased Aβ and tau pathologies in 3xTg-AD mice by affecting BACE1 and NEP expression. These results indicated that OXA aggravates cognitive deficits and hippocampal synaptic plasticity impairment in 3xTg-AD mice by increasing Aβ production and decreasing Aβ clearance through disruption of the circadian rhythm and sleep-wake cycle.

1. Introduction

The main clinical feature of Alzheimer's disease (AD), an irreversible neurodegenerative disease, is dementia characterized by noticeable memory, language, thinking or behavioral symptoms (Alzheimer's disease facts and figures, 2022). According to the World Alzheimer's Disease Report 2021, approximately 55 million people have dementia worldwide, more than 2 of 3 whom have AD (Serge et al., 2021). The pathogenesis of AD is very complicated. The typical pathological features of AD are extracellular amyloid β (Aβ) plaques and intracellular neurofibrillary tangles (NFTs) containing abnormally phosphorylated tau. Studies in both AD patients and animal models have demonstrated the neurotoxicity of Aβ (Sciaccaluga et al., 2021; Tolar et al., 2021), and the amyloid hypothesis fits reasonably well the autosomal dominant AD which exhibits mutations in presenilin (PSEN) 1, PSEN2 and β-amyloid precursor protein (APP) (Frisoni et al., 2022). Moreover, the bilateral delivery of synthetic Aβ oligomers into the cerebral parenchyma in cynomolgus monkeys induces a cascade of pathological events resembling the early phase of AD in humans (Yue et al., 2021), thus providing experimental evidence from non-human primates supporting the amyloid cascade hypothesis. However, increasing evidence indicates that the synergy between Aβ and tau plays an important role in AD pathogenesis (Busche and Hyman, 2020). Although Aβ may initiate the cascade of events, tau impairment is likely the effector molecule of neurodegeneration (Roda et al., 2022), which indicates the importance of using AD model mice that exhibit both plaque and tangle pathologies.

Orexins/hypocretins are neuropeptides that are specifically synthesized by orexinergic neurons in the lateral hypothalamus, which have extensive projections to other wakefulness-promoting neurons and play crucial roles in the induction and maintenance of wakefulness (Jacobson et al., 2022; Liu and Dan, 2019). The 2 structural forms of orexin are orexin-A (OXA) and orexin-B (OXB). OXA is completely structurally conserved among several mammalian

* Correspondence authors at: Department of Physiology, Shanxi Medical University, Taiyuan, Shanxi, China, Tel: +86 351 4135117.
E-mail addresses: caojimin@sxmu.edu.cn (J.-M. Cao), wmna@163.com (M.-N. Wu).

0197-4580/$ – see front matter © 2023 Elsevier Inc. All rights reserved.
https://doi.org/10.1016/j.neurobiolaging.2023.01.008

species (human, rat, mouse, cow, sheep, dog and pig), whereas the amino acid sequence of OXB is not (Jacobson et al., 2022). OXA is closely related to the pathogenesis of AD (Wang et al., 2018). Patients with mild cognitive impairment (MCI) exhibit abnormally elevated OXA levels in cerebrospinal fluid (CSF), along with reduced rapid eye movement (REM) sleep, lower $A\beta_{1\text{-}42}$ levels and increased phosphorylated tau in CSF (Liguori et al., 2016). Similarly, AD patients show increases in OXA and phosphorylated tau levels and higher t-tau/$A\beta_{1\text{-}42}$ ratios (an index of marked neurodegeneration) in the CSF, as well as significantly lower minimental state examination (MMSE) scores (an indicator of cognitive function) and sleep-wake pattern disruption (Gabelle et al., 2017; Liguori et al., 2017; Liguori et al., 2019; Liguori et al., 2014). In Tg2576 mice, intracerebroventricular (i.c.v.) injection of OXA increases $A\beta$ levels in the interstitial fluid of the hippocampus by prolonging wakefulness (Kang et al., 2009). Furthermore, a recent study of APP/PS1 mice, which mainly exhibit $A\beta$ plaques, found that chronic i.c.v. injection of OXA increases $A\beta$ levels and impairs spatial learning and memory (Li et al., 2020). However, no study has examined the impact of exogenous OXA on other types of cognitive deficits in mouse models of AD, especially in 3xTg-AD mice exhibiting both plaque and tangle pathologies (Oddo et al., 2003). In particular, whether OXA treatment affects tau phosphorylation and enzymes related to $A\beta$ metabolism is unclear.

Synaptic plasticity in the hippocampus is the electrophysiological basis of animal learning and memory behaviors, and long-term potentiation (LTP) is an important cellular model of synaptic plasticity (Dringenberg, 2020). We and others have observed LTP depression in the hippocampus in 3xTg-AD mice both in vitro and in vivo, suggesting an electrophysiological basis of cognitive impairment (Cai et al., 2021; Oddo et al., 2003; Yan et al., 2022). OXA administration significantly increases the spontaneous firing rate of hippocampal CA1 neurons in rats (Chen et al., 2017), induces state-dependent LTP of synaptic transmission at Schaffer collateral-CA1 synapses in hippocampal slices in vitro (Selbach et al., 2010) and bidirectional modulates hippocampal CA1 synaptic plasticity in vitro (Lu et al., 2016). However, the impact of OXA on synaptic plasticity in mouse models of AD has not been comprehensively examined.

To contribute to addressing the gaps outlined above, the present study aimed to investigate the mechanisms by which OXA impairs synaptic plasticity, increases $A\beta$ plaques and NFTs, and ultimately aggravates cognitive defects in 3xTg-AD mice. We first observed the effects of OXA treatment on multiple cognitive deficits in this mouse model, which exhibits an age-related and progressive neuropathological phenotype involving both $A\beta$ and tau pathologies. We then performed in vivo hippocampal electrophysiological recording to investigate the potential electrophysiological mechanism by which OXA aggravates cognitive deficits. We further explored the effects of OXA on tau phosphorylation and $A\beta$ metabolism in the brain in 3xTg-AD mice, including enzymes involved in the production and degradation of $A\beta$. In addition, the effects of OXA on the circadian locomotor rhythm and sleep-wake cycle were observed by monitoring wheel-running activity.

2. Materials and methods

2.1. Animals and treatment

Homozygous APP/PS1/tau triple-transgenic AD (3xTg-AD) model mice (stock number: 034830-JAX, Jackson Laboratory, USA) (Oddo et al., 2003) and age-matched C57B6/129 wild-type (WT) mice with the same genetic background were used. All animal procedures were performed in accordance with the guidelines established by the Ethics Committee for the Use of Experimental Animals at Shanxi Medical University. Mice were housed under a 12 hour:12 hour light-dark cycle (lights on at 06:00 and off at 18:00) with controlled room temperature (20–24°C) and humidity (50%–60%) and received standard rodent chow and water. Because females have a higher risk of developing AD (Eissman et al., 2022) and estradiol and progesterone levels affect $A\beta$ levels in transgenic mouse models of AD (Li and Singh, 2014), only male 3xTg-AD mice were used in the present study to avoid the influence of sex differences. Twelve-month-old male 3xTg-AD mice and WT mice (all specific-pathogen-free (SPF)) were randomly divided into 4 groups: WT + Vehicle (n = 15), WT+OXA (n = 15), 3xTg-AD+Vehicle (n = 15) and 3xTg-AD + OXA (n = 16). During the initial 1-week adaptation period, each mouse was intranasal administered deionized water daily at 18:00 (the beginning of the mouse activity period). Next, each mouse was intranasal administered 0.8 nmol of OXA (Tocris, UK) or the same volume of deionized water (vehicle) daily for 14 days at 18:00 (Yang et al., 2013). After the 14-day treatment period, cognitive behavioral experiments were performed, and daily drug or vehicle administration was continued until the mice were sacrificed (Fig. 1).

2.2. Behavioral tests

As mice are nocturnal, all behavioral experiments were conducted in the active phase (dark phase) under dim red light (<10 lux) to avoid affecting the physiological condition and sleep-wake cycle of the mice (Zhang et al., 2017). To eliminate the effect of odor on the experimental results, the object recognition experimental box and the Y-maze were wiped with 75% ethanol between experimental sessions.

2.2.1. Novel object recognition test

The recognition memory of the mice was evaluated by performing the novel object recognition test (NORT), which exploits the natural tendency of rodents to explore novel objects (Dionisio-Santos et al., 2021). The experimental box was a cube with a length, width and height of 40 cm. An infrared camera was used to record the original traces, and Smart 3.0 software (Panlab Harward Apparatus, USA) was used to analyze the data. The mice were adapted in the behavioral laboratory and open field for 1 day. First, 2 identical objects were placed in the experimental box, and each mouse was allowed to explore freely for 10 minutes. Six hours later, one of the objects was replaced with a novel object, and each mouse was returned to the same position in the box and allowed to explore the box for 10 minutes. The exploration times of the familiar object and novel object were recorded, and the object recognition index (RI) and discrimination index (DI) were calculated as follows: RI = [time exploring the novel object/total time exploring both objects] × 100%; DI = [(time exploring the novel object - time exploring the familiar object)/total time exploring both objects] × 100%. This test assumes that when both objects are unfamiliar, the chance that the mouse will explore a specific object is determined by random chance (50%). When one object is familiar, the mouse will spend more time exploring the novel object, and its RI will be higher than 50%. Thus, an RI below 50% is interpreted as a lack of discrimination between the novel object and the familiar object (Fanet et al., 2021).

2.2.2. Y-maze spontaneous alternation test

The Y-maze spontaneous alternation test (YMT) was used to evaluate short-term spatial working memory, which is the memory function of temporarily processing and storing information (Kraeuter et al., 2019). The Y-maze consisted of 3 arms (length of 30 cm, width of 5 cm and height of 15 cm) that met at angles of 120°. The test was initiated by placing a mouse in the center of the

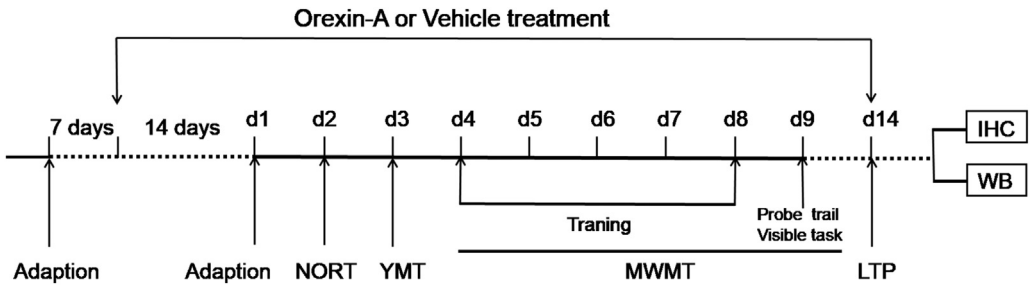

Fig. 1. Schematic diagram of the experimental procedure. After 7 days of adaptation to the laboratory environment and intranasal administration, orexin-A (OXA) or vehicle was intranasal administered once daily for 14 days before the behavioral tests. The drug treatment was maintained during all behavioral tests, including the novel object recognition test (NORT), Y maze spontaneous alternation test (YMT) and Morris water maze test (MWMT). Following the behavioral tests, in vivo hippocampal long-term potentiation (LTP) recording, immunohistochemistry (IHC) and western blotting were performed.

maze and allowing it to explore the 3 arms freely for 8 minutes. The total number of arm entries and the order of arm exploration were recorded. The percentage of correct spontaneous alternations was calculated as [(number of correct alternations)/(total arm entries - 2)] $\times$ 100%.

2.2.3. Morris water maze test

Spatial learning and memory were evaluated using the Morris water maze test (MWMT) as described in our previous study (Zhou et al., 2020). The water maze was a circular swimming pool (diameter of 120 cm and height of 50 cm) with a small escape platform (diameter of 12 cm). The maze was divided into 4 equal quadrants, and the escape platform was placed 1 cm below the water surface in the center of the first quadrant. Differently shaped visual cues were positioned at the inner wall of the pool. During the experiments, the water temperature was maintained at 23°C $\pm$ 2°C.

In the hidden platform test, each mouse was tested 4 times daily for 5 consecutive days. The mouse had a maximum of 60 seconds per trial to find the escape platform underwater depending on the visual cues around the maze. Each trial began with the mouse entering the water from the midpoint of 1 quadrant and ended when the mouse found the hidden platform or after 60 seconds. Once the mouse climbed onto the platform, it was allowed to stay for 30 seconds to observe the surrounding environment. If the mouse did not find the platform within 60 seconds, it was manually guided to the platform and allowed to stay for 30 seconds to familiarize itself with and remember the surroundings or cues. The escape latency on each training day was determined by taking the average of the 4 trials. On the sixth day, the probe test was performed to evaluate memory retention ability. During the probe test, the platform was removed, and the searching behavior of the mouse in the target quadrant (where the platform was located during the hidden platform training) was observed. The swimming speed, swimming trajectory, and swimming time of the mouse in each quadrant and the number of crossings were recorded and analyzed by a video tracking system (Ethovision 3.0, Noldus Information Technology, Wageningen, Netherlands). In addition, to examine the vision and motor ability of each mouse, a visible platform test was conducted in which the time of arrival at a platform 1 cm above the water surface was recorded.

2.3. In vivo hippocampal electrophysiological recording

Synaptic plasticity is closely related to cognitive function (Bliss and Collingridge, 1993). After the behavioral experiments, in vivo electrophysiological recording was performed. Each mouse was anesthetized with 5% chloral hydrate (0.08 ml/10 g, i.p.) and placed on a stereotaxic apparatus (68016, RWD Life Science, China). A dental drill was employed to make a small hole (2.0 mm posterior to the bregma and 1.5 mm lateral to the midline) in the skull, and stimulating/recording electrodes were located at the Schaffer collateral/commissural pathway and the stratum radiatum of the hippocampal CA1 region. First, field excitatory postsynaptic potentials (fEPSPs) were evoked by stimuli of increasing amplitude (0–0.3 mA in 0.02 mA increments; duration: 50 μs) at a frequency of 0.033 Hz, and the input–output (I/O) curve was drawn. Based on the I/O curve, baseline fEPSPs were evoked by test stimulation (intensity, 50% of maximal fEPSPs; frequency, 0.033 Hz) delivered to the Schaffer-collateral/commissural pathway and recorded for 30 minutes; then, paired-pulse facilitation (PPF) was induced by 2 stimuli with an interval of 50 ms. Finally, high-frequency stimulation (HFS) was applied to induce LTP. The HFS protocol consisted of 3 trains of 20 stimuli at 200 Hz with an intertrain interval of 30 seconds. After HFS, the test stimuli were used again for at least 1 hour to record any change in the slope of the fEPSPs (Yan et al., 2022).

2.4. Immunohistochemistry

After electrophysiological recording, mice were randomly selected from each group and slowly perfused with saline solution and 4% paraformaldehyde solution. Then, the brain was removed from the skull and immersed in 4% paraformaldehyde (4°C) overnight. The brain tissue was gradient dehydrated by sequential immersion in 15% and 30% sucrose solutions, flash frozen in liquid nitrogen for 20 seconds and sliced with a thickness of 10 μm at -20°C using a cryostat microtome (CM1850, Leica, Germany). Aβ plaques and tau hyperphosphorylation in the mouse hippocampus and cortex were detected in coronal sections stained with mouse monoclonal anti-amyloid 1–16 (6E10, 803015, 1:750, Biolegend, USA) and rabbit polyclonal antibody anti-tau (phospho T231, ab151559, 1:200, Abcam, UK). The immunostained sections were imaged by optical microscopy (BX51, Olympus, Japan). The mean percentage area of antigen-antibody complexes was measured using ImagePro Plus 6.0 (Fryer, Huntley, IL, USA).

2.5. Western blotting

Bilateral hippocampi were removed from mice randomly selected from each group and weighed. The tissues were homogenized using an ultrasonic homogenizer in cold RIPA buffer (AR0102, Boster, China) containing a cocktail of phenylmethylsulfonyl fluoride (PMSF; AR1179, Boster, China) and protein phosphatase inhibitor (AR1183, Boster, China). Then, the lysates were centrifuged at 13,000 r/min for 15 minutes. The protein concentration of the supernatant was measured using a bicinchoninic acid protein kit (AR0146, Boster, China). The total protein samples were diluted

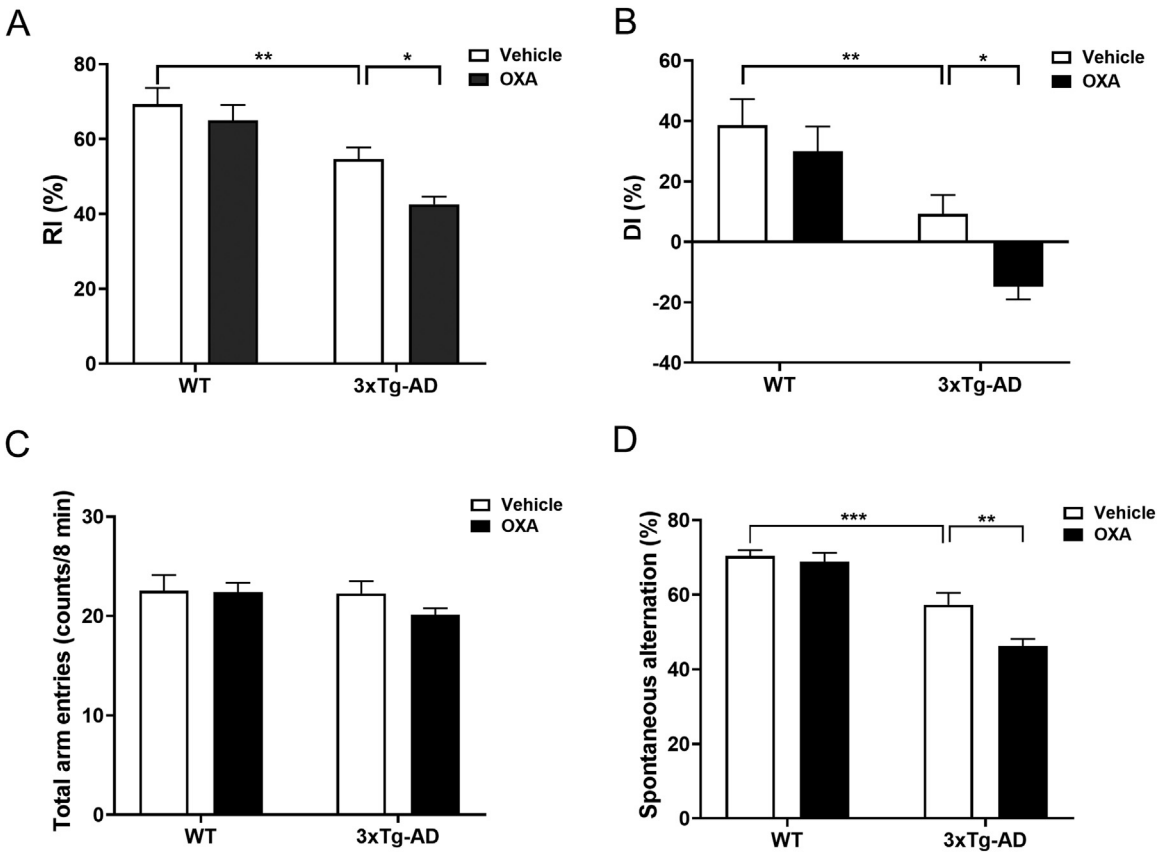

Fig. 2. OXA aggravated the impairments of recognition memory and working memory in 3xTg-AD mice. (A and B) Bar plots showing the RI and DI of each group of mice in the novel object recognition test (NORT). (C-D) Bar plots showing the total number of arm entries and the percentage of correct spontaneous alternations of each group of mice in the Y-maze spontaneous alternation test (YMT) (n = 15–16, $^{*}p < 0.05$, $^{**}p < 0.01$, $^{***}p < 0.001$).

1:1 with loading buffer (AR0131, Boster, China) and boiled for 5 minutes at 95°C–100°C. The protein samples (30–50 μg) were then separated by electrophoresis on a 12% SDS-polyacrylamide gel and transferred to a PVDF membrane (Millipore, USA). The membrane was incubated with 5% defatted milk powder (D8340, Solarbio, China) or 5% BSA blocking buffer (SW3015, Solarbio, China) at room temperature for 2 hours. Next, the membrane was incubated at 4°C overnight with primary antibodies (β-actin, 1:5000, D191047, Sangon Biotech, China; GAPDH, 1:5000, AP0063, Bioworld Technology, USA; anti-Aβ, 6E10, 1:10000, Biolegend, USA; anti-BACE1, 1:1000, ab2077, Abcam, UK; anti-Neprilysin-2, 1:1000, ab81688, Abcam, UK; anti-phospho-Tau (Ser202, Thr205) (AT8), 1:1000, MN1020, Thermo Fisher Scientific, USA; anti-phospho-tau (T231), 1:1000, ab151559, Abcam, UK; anti-Tau (Tau5), 1:1000, ab80579, Abcam, UK), followed by the secondary antibody (anti-rabbit IgG, 1:5000, BA1054, Boster, China; anti-mouse IgG, 1:5000, BA1050, Boster, China) for 2 hours at room temperature. Finally, the immunocomplex was visualized by enhanced chemiluminescence and detected by ImagePro Plus 6.0 (Fryer, Huntley, IL, USA).

2.6. Recording of wheel running activity

To evaluate the behavioral circadian rhythm of the mice, the wheel-running activity of randomly selected 3xTg-AD mice and WT mice treated with OXA or vehicle (n = 4 for each group) was recorded. Each mouse was housed individually in cages within chambers equipped with LED lights and maintained under a 12 hour:12 hour light-dark cycle (lights on at 06:00 and off at 18:00) for 2 weeks. All activity data were recorded in 5 minute bins using ClockLab software Version 6 (Actimetrics Inc., USA). The period, amplitude, robustness, interdaily stability (IS) and intradaily variability (IV) were analyzed using ClockLab software and software available at http://www.circadian.org/softwar.html, and the locomotor activity was measured and statistically quantified (Wu et al., 2018).

2.7. Statistical analysis

All data are presented as the mean ± standard error. The escape latency in the MWMT was analyzed by 3-factor repeated-measures analysis of variance (ANOVA), the 6E10^{+} area in immunohistochemical staining was analyzed by the 2-sample t test, and all other data were analyzed using two-way ANOVA and Tukey's post hoc test. GraphPad Prism 9.0 and SigmaPlot 14.0 were used to analyze the data, and $p < 0.05$ was considered statistically significant.

3. Results

3.1. OXA aggravated the impairments of recognition memory and working memory in 3xTg-AD mice

In the NORT (Fig. 2A and B), the recognition index (RI) was 69.3% ± 4.3% in the WT+Vehicle group and decreased to 54.6% ± 3.1% in the 3xTg-AD + Vehicle group ($p = 0.005$), and OXA treatment further decreased the RI of 3xTg-AD mice to 42.6% ± 2.1% ($p = 0.017$). The discrimination indexes (DIs) in the WT + Vehi-

cle group, WT+OXA group, 3xTg-AD + Vehicle group and 3xTg-AD + OXA group were 38.6%±8.7%, 30.0% ± 8.1%, 9.2% ± 6.3% and -14.9% ± 4.2%, respectively. Compared with the WT + Vehicle group, the 3xTg-AD + Vehicle group exhibited a significant reduction in the DI ($p = 0.005$), and OXA treatment further reduced the DI of 3xTg-AD mice ($p = 0.017$) (two-way ANOVA: genotype: $F_{(1, 60)} = 28.450$, $p < 0.001$; treatment: $F_{(1, 60)} = 5.520$, $p = 0.022$; genotype × treatment: $F_{(1, 60)} = 1.251$, $p = 0.268$). These results indicated that recognition memory was impaired in 12-month-old 3xTg-AD mice and that OXA treatment further aggravated this impairment in 3xTg-AD mice.

In the YMT (Fig. 2C and D), there was no significant difference in total arm entries among the 4 groups (two-way ANOVA: genotype: $F_{(1, 60)} = 1.244$, $p = 0.269$; treatment: $F_{(1, 60)} = 0.996$, $p = 0.322$; genotype×treatment: $F_{(1, 60)} = 0.776$, $p = 0.382$). However, the percentage of correct spontaneous alternation was significantly lower in the 3xTg-AD+Vehicle group (57.3% ± 3.2%) than in the WT + Vehicle group (70.4% ± 1.6%, $p < 0.001$), and OXA treatment further decreased the percentage to 46.3% ± 1.9% in the 3xTg-AD+OXA group ($p = 0.001$). (two-way ANOVA: genotype: $F_{(1, 60)} = 59.214$, $p < 0.001$; treatment: $F_{(1, 60)} = 7.370$, $p = 0.009$; genotype × treatment: $F_{(1, 60)} = 4.213$, $p = 0.045$). These results indicated that OXA treatment obviously aggravated the working memory impairment of 3xTg-AD mice without affecting locomotor activity.

3.2. OXA exacerbated the impairments of spatial learning and memory in 3xTg-AD mice

In the hidden platform test (Fig. 3A and B) of the MWMT, the escape latency of all 4 groups of mice gradually decreased as the number of training days increased (repeated-measures ANOVA: day: $F_{(4, 285)} = 28.48$, $p < 0.001$). Nonetheless, the average escape latency was greater in the 3xTg-AD+Vehicle group than in the WT + Vehicle group on day 3 ($p = 0.030$), and OXA treatment further prolonged the escape latency of 3xTg-AD mice on day 3 ($p = 0.028$) and day 5 ($p = 0.040$), indicating that OXA treatment aggravated the impairment of spatial learning ability in 3xTg-AD mice. In addition, OXA treatment prolonged the escape latency of WT mice on day 4 ($p = 0.014$), indicating that OXA treatment also impaired the spatial learning ability of WT mice (two-way ANOVA: day 3: genotype: $F_{(1, 60)} = 13.721$, $p < 0.001$; treatment: $F_{(1, 60)} = 6.918$, $p = 0.011$; genotype × treatment: $F_{(1, 60)} = 0.279$, $p = 0.599$; day 4: genotype: $F_{(1, 60)} = 3.436$, $p = 0.069$; treatment: $F_{(1, 60)} = 10.082$, $p = 0.002$; genotype × treatment: $F_{(1, 60)} = 0.208$, $p = 0.650$; day 5: genotype: $F_{(1, 60)} = 4.841$, $p = 0.032$; treatment: $F_{(1, 60)} = 8.196$, $p = 0.006$; genotype × treatment: $F_{(1, 60)} = 0.008$, $p = 0.928$).

In the probe test (Fig. 3C–E) on day 6, the APP/PS1/tau gene mutation and OXA treatment both had main effects on the percentage of swimming time in the target quadrant (two-way ANOVA: genotype: $F_{(1, 60)} = 8.176$, $p = 0.006$; treatment: $F_{(1, 60)} = 9.651$, $p = 0.003$; genotype × treatment: $F_{(1, 60)} = 0.169$, $p = 0.683$) and the number of platform crossings (two-way ANOVA: genotype: $F_{(1, 60)} = 18.384$, $p < 0.001$; treatment: $F_{(1, 60)} = 10.319$, $p = 0.002$; genotype×treatment: $F_{(1, 60)} = 0.134$, $p = 0.716$). The percentage in the target quadrant was significantly lower in the 3xTg-AD + Vehicle group (44.3% ± 2.8%) than in the WT + Vehicle group (57.5% ± 3.9%, $p = 0.026$), and OXA treatment further reduced the percentage to 33.3% ± 2.9% in the 3xTg-AD + OXA group ($p = 0.06$). The number of platform crossings was also significantly lower in the 3xTg-AD+Vehicle group than in the WT+Vehicle group ($p = 0.008$), and OXA treatment further decreased the number of platform crossings in the 3xTg-AD + OXA group ($p = 0.014$). In addition, OXA treatment decreased the swimming time percentage ($p = 0.017$) and number of platform crossings ($p = 0.051$) in the WT+OXA group compared with the WT + Vehicle group. These results indicated that OXA treatment aggravated the spatial memory impairment of 3xTg-AD mice and impaired the spatial memory of WT mice.

In the visual platform test, there was no significant difference in the time to reach the platform among the 4 groups ($p > 0.05$, Fig. 3F), and there was no significant difference in swimming speed among the 4 groups throughout the experiment ($p > 0.05$, Fig. 3G). The above results indicated that the APP/PS1/tau gene mutation and OXA treatment did not affect the vision and motor ability of the mice; thus, the prolonged escape latency and decreases in swimming time percentage and number of platform crossings observed in both 3xTg-AD mice and WT mice after OXA treatment were the result of impairments in long-term spatial learning and memory.

3.3. OXA damaged hippocampal synaptic plasticity in 3xTg-AD mice

It is widely believed that changes in synaptic plasticity form the cellular basis of learning and memory (Diering and Huganir, 2018). To evaluate synaptic plasticity in WT and 3xTg-AD mice, basic synaptic transmission and HFS-induced LTP in the hippocampal CA1 region were recorded. The results showed that with increasing stimulus intensity, the fEPSP amplitude gradually increased in all 4 groups of mice; under the same stimulus intensity, the fEPSP amplitude did not differ significantly among the 4 groups ($p > 0.05$, Fig. 4A). In addition, the fEPSP slopes evoked by the test stimulus were relatively stable, with no significant difference among the 4 groups of mice within 30 minutes of recording ($p > 0.05$, Fig. 4C and D). These results indicated that the APP/PS1/tau gene mutation and OXA treatment did not affect basic synaptic transmission in the hippocampus. After paired pulse stimulation, the PPF value (fEPSP2/fEPSP1) was not significantly different among the 4 groups of mice ($p > 0.05$, Fig. 4B), demonstrating that the different genotypes and drug treatments did not affect presynaptic neurotransmitter release.

After high-frequency stimulation (HFS), the fEPSP slopes in the WT+Vehicle group, WT+OXA group, 3xTg-AD+Vehicle group and 3xTg-AD+OXA group immediately increased to 176.0% ± 2.5%, 171.6% ± 2.4%, 160.6% ± 3.6% and 155.0% ± 4.3%, respectively, indicating that HFS successfully induced LTP in each group. At 0 minute, 30 minute and 60 minute after HFS (Fig. 4C–E), the fEPSP slope was significantly lower in the 3xTg-AD+Vehicle group than in the WT + Vehicle group ($p < 0.001$). Furthermore, OXA treatment decreased the fEPSP slopes of 3xTg-AD mice and WT mice at 30 minute and 60 minute after HFS ($p < 0.001$). (two-way ANOVA: 0 minute: genotype: $F_{(1, 25)} = 48.355$, $p < 0.001$; treatment: $F_{(1, 25)} = 5.323$, $p = 0.031$; genotype×treatment: $F_{(1, 25)} = 0.004$, $p = 0.953$; 30 minute: genotype: $F_{(1, 25)} = 185.635$, $p < 0.001$; treatment: $F_{(1, 25)} = 35.295$, $p < 0.001$; genotype×treatment: $F_{(1, 25)} = 0.130$, $p = 0.722$; 60 minute: genotype: $F_{(1, 25)} = 286.978$, $p < 0.001$; treatment: $F_{(1, 25)} = 69.639$, $p < 0.001$; genotype×treatment: $F_{(1, 25)} = 0.996$, –0.329). These results indicated that hippocampal synaptic plasticity was impaired in 3xTg-AD mice and that OXA treatment exacerbated this impairment in 3xTg-AD mice and induced synaptic plasticity impairment in WT mice.

3.4. OXA increased Aβ plaques and soluble Aβ oligomers in the hippocampus and cortex in 3xTg-AD mice

The deposition of Aβ plaques is an important pathological characteristic of AD. In this study, Aβ plaques in the hippocampus and cortex were observed by immunohistochemical staining. As

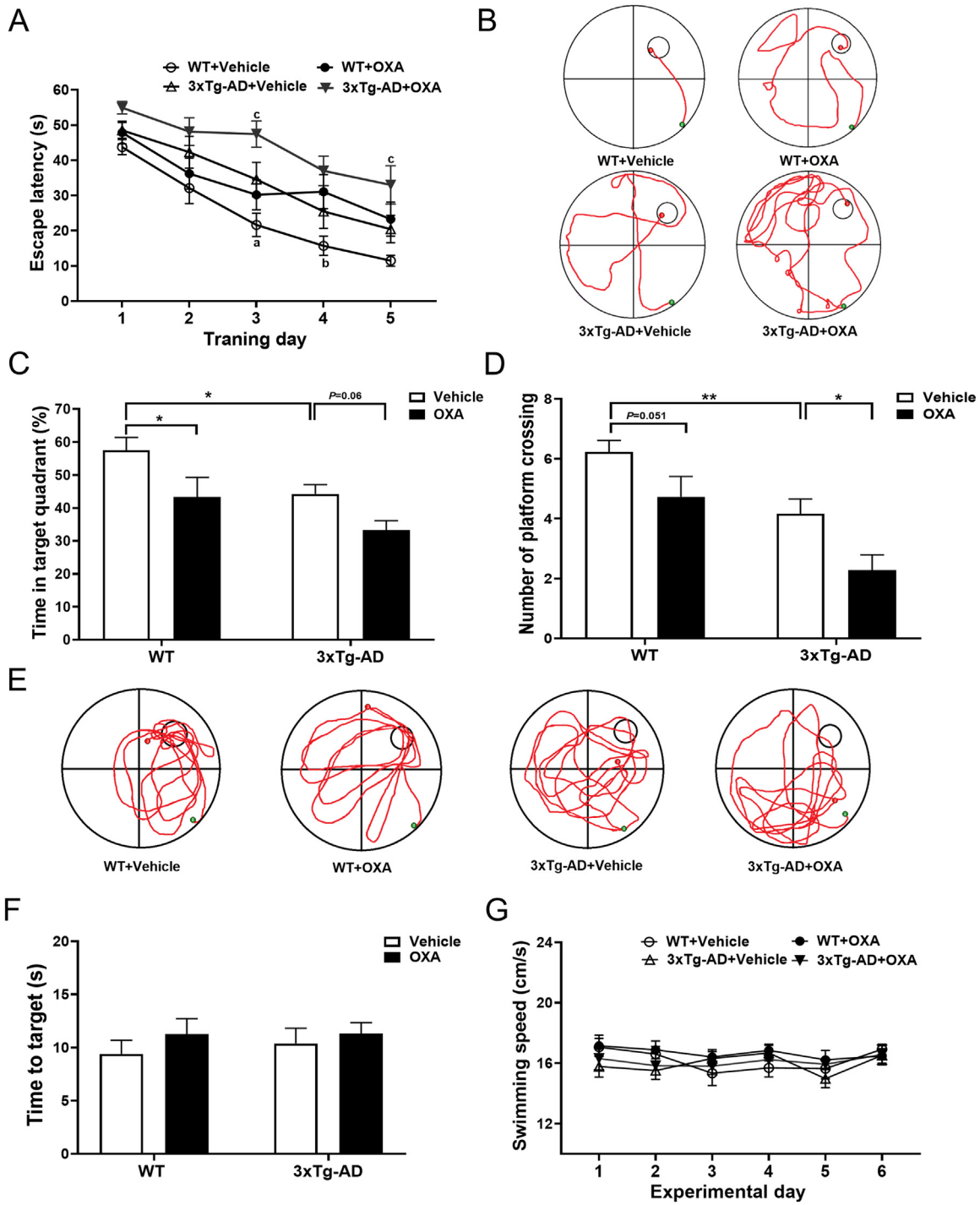

Fig. 3. OXA exacerbated the impairments of long-term spatial learning and memory in 3xTg-AD mice. (A) Line charts showing the escape latency of mice in the hidden platform test of the Morris water maze test (MWMT) over 5 consecutive training days ([a]WT + Vehicle group vs. 3xTg-AD + Vehicle group, $p < 0.05$; [b]WT + Vehicle group vs. WT + OXA group, $p < 0.05$; [c]3xTg-AD + Vehicle group vs. 3xTg-AD + OXA group, $p < 0.05$). (B) Representative swimming trajectories of mice in each group on day 5. The large circle represents the water maze pool, and the small circle represents the hidden platform. The green and red points indicate the beginning and end of one experimental trial, respectively. (C) Bar plots showing the percentage of swimming time in the target quadrant of each group of mice on day 6. (D) Bar plots showing the number of platform crossings in the probe test on day 6. (E) Representative swimming trajectory diagrams of each group of mice in the probe test. (F) The time of arrival of each group of mice at the platform in the visual platform test. (G) Line charts of the swimming speeds of the 4 groups of mice on days 1–6 (n = 15–16, $^{*}p < 0.05$, $^{**}p < 0.01$) (For interpretation of the references to color in this figure legend, the reader is referred to the Web version of this article.)

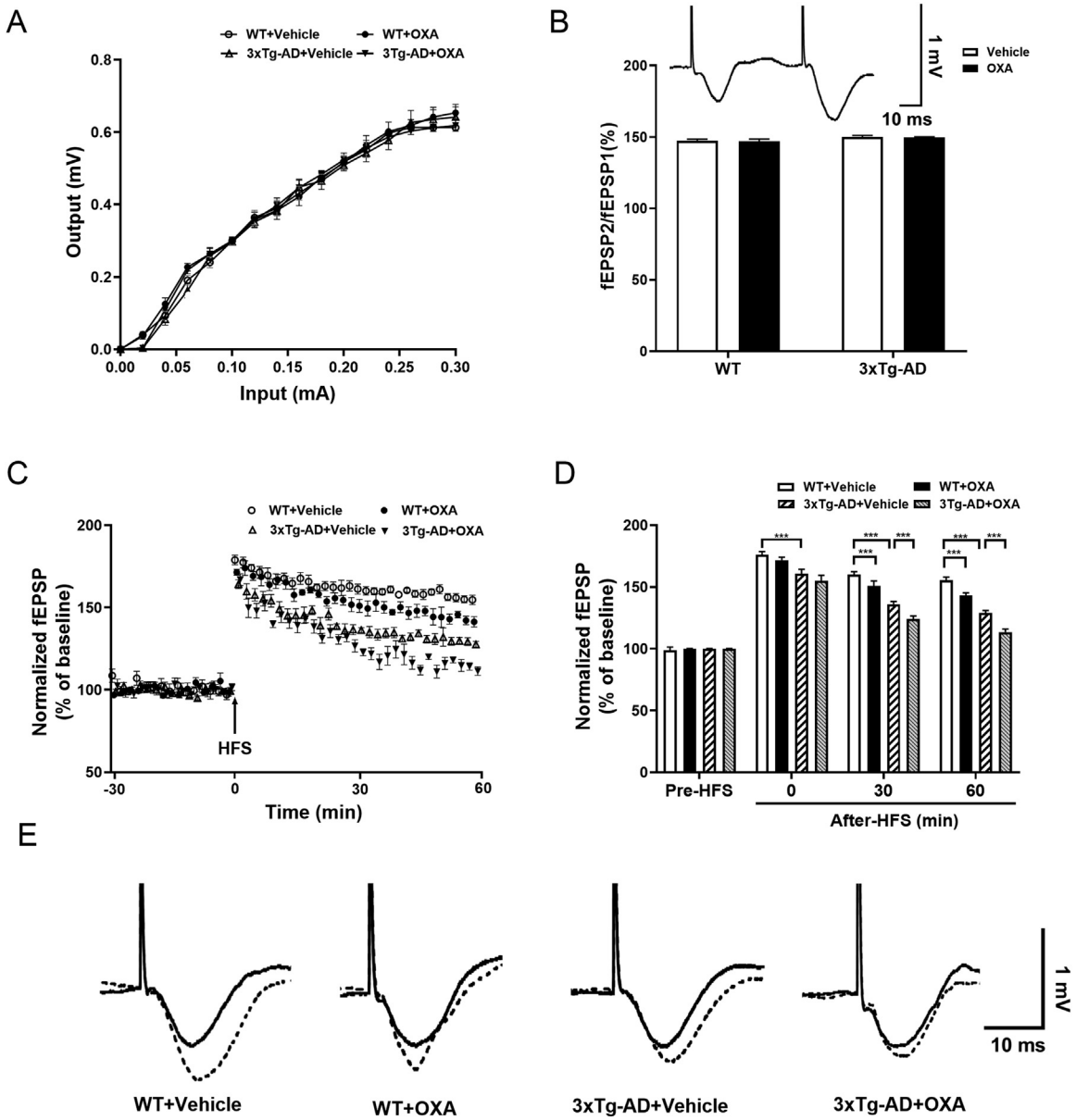

Fig. 4. OXA damaged hippocampal LTP in 3xTg-AD mice. (A) There was no significant difference in the I-O curves among the 4 groups. (B) Bar plots showing the PPF values among the 4 groups. (C) Time course of fEPSP slopes and LTP induced by HFS in the hippocampus. (D) Bar plots showing the fEPSP slopes of the mice before and 0 minute, 30 minute and 60 minute after HFS. (E) Representative fEPSP traces of the 4 groups before (solid line) and 60 minute after HFS (dashed line) (n = 6-8, *** $p < 0.001$).

shown in Fig. 5A–C, scattered Aβ plaques were observed in the hippocampus and cortex in 3xTg-AD mice, and OXA treatment increased the area of Aβ-positive plaques in the hippocampus (t = -4.749, $p = 0.001$) and cortex (t = -6.297, $p < 0.001$) in 3xTg-AD mice.

As the neurotoxicity of Aβ is mainly due to soluble Aβ oligomers (Reiss et al., 2018; Tolar et al., 2021), the level of Aβ oligomers in the hippocampus in 3xTg-AD mice was assessed (Fig. 5D and E). The results showed that the APP/PS1/tau gene mutation and OXA treatment both had main effects on the level of Aβ oligomers (two-way ANOVA: genotype: $F_{(1, 15)} = 31.095$, $p < 0.001$; treatment: $F_{(1, 15)} = 6.220$, $p = 0.028$; genotype×treatment: $F_{(1, 15)} = 2.810$, $p = 0.120$). The level of Aβ oligomers in the hippocampus was significantly higher in the 3xTg-AD+Vehicle group than in the WT+Vehicle group ($p = 0.018$), and OXA treatment obviously increased the level of Aβ oligomers in 3xTg-AD mice ($p = 0.012$).

3.5. OXA affected the expression of Aβ metabolism-related enzymes in the hippocampus in 3xTg-AD mice

Aβ is the cleavage product of APP, and β-site amyloid precursor protein cleaving enzyme 1 (BACE1) is the enzyme that initiates the generation of Aβ (Hampel et al., 2021). In addition, neprilysin (NEP) plays an important role in the degradation of Aβ monomers and oligomers (Campos et al., 2020). To investigate the mechanisms underlying the increases in Aβ oligomers and plaques in the brain in 3xTg-AD mice after OXA treatment, the expression levels of BACE1 and NEP in the hippocampus were measured. As shown in Fig. 6, the expression levels of BACE1 ($p < 0.001$) and NEP ($p = 0.016$) in the hippocampus were significantly higher in the 3xTg-AD+Vehicle group than in the WT + Vehicle group. After OXA treatment, the expression level of BACE1 further increased in 3xTg-AD mice ($p = 0.028$), whereas the expression level of NEP significantly decreased ($p = 0.011$) (two-way ANOVA: BACE1:

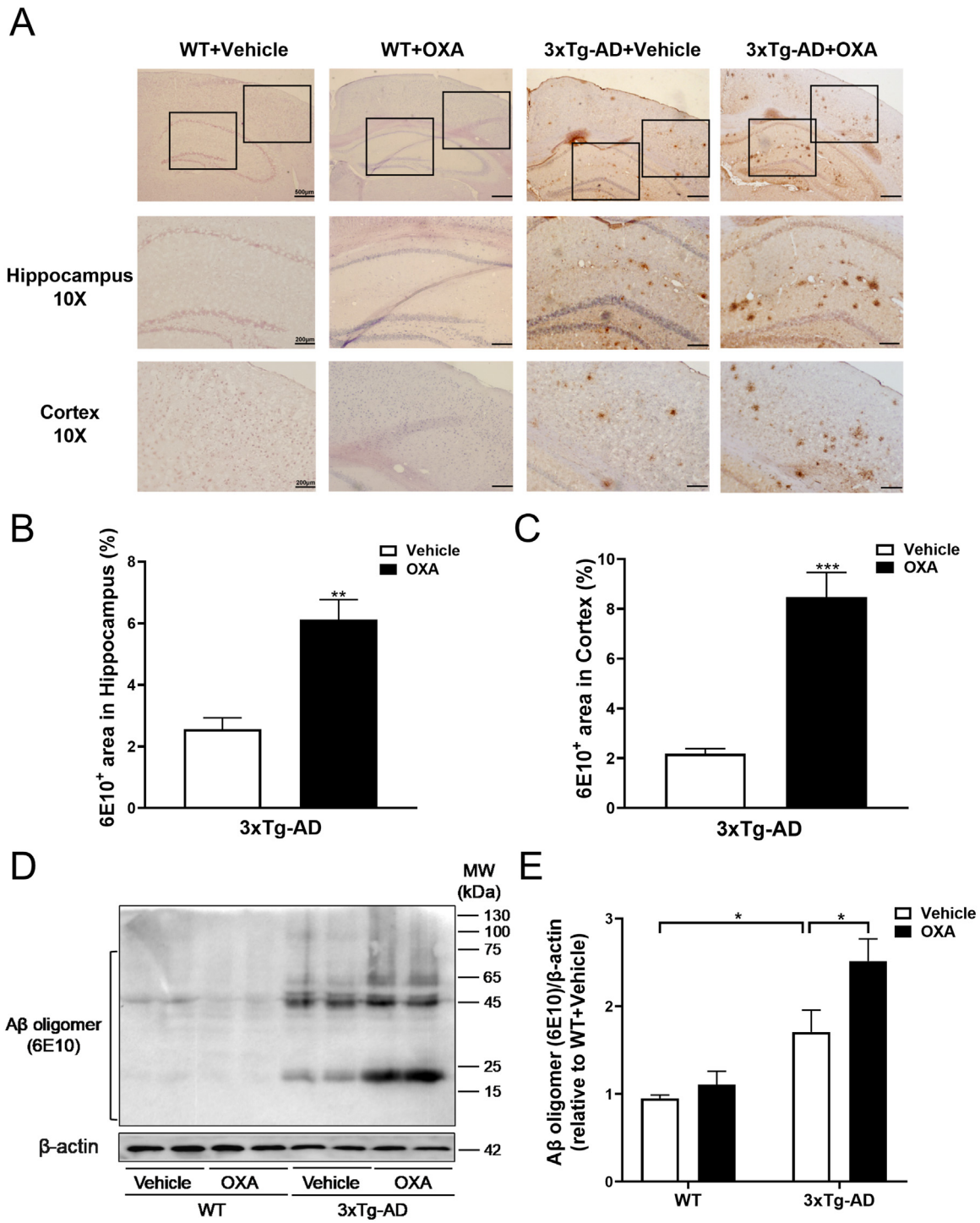

Fig. 5. OXA increased Aβ deposition and soluble Aβ oligomers in the brain in 3xTg-AD mice. (A) Representative images of immunohistochemical staining of Aβ plaques in the hippocampus and cortex in the 4 groups of mice. (B–C) Bar plots showing the percentage of 6E10 immunopositive area in the hippocampus and cortex in 3xTg-AD mice (n = 5, $^{**}p < 0.01$, $^{***}p < 0.001$). (D) Representative original immunoblots of Aβ oligomers in the hippocampus. (E) Bar plots showing the expression level of Aβ oligomers in the hippocampus (n = 4, $^{*}p < 0.05$).

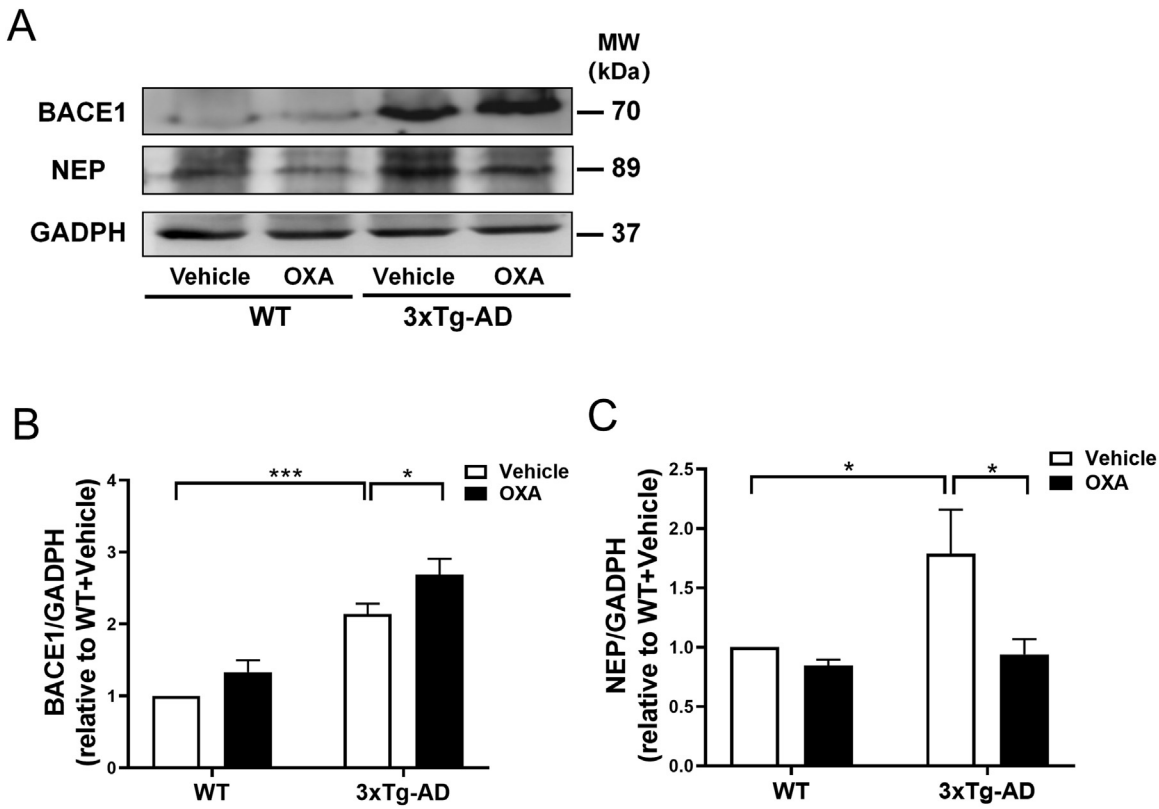

Fig. 6. OXA affected the expression of BACE1 and NEP in the hippocampus in 3xTg-AD mice. (A) Representative original immunoblots of BACE1 and NEP expression in the hippocampus. (B–C) Bar plots showing the expression levels of BACE1 and NEP in the hippocampus (n = 4, $^{*}p < 0.05$, $^{***}p < 0.001$).

genotype: $F_{(1, 15)} = 64.366$, $p < 0.001$; treatment: $F_{(1, 15)} = 8.041$, $p = 0.015$; genotype×treatment: $F_{(1, 15)} = 0.481$, $p = 0.501$; NEP: genotype: $F_{(1, 15)} = 4.902$, $p = 0.047$; treatment: $F_{(1, 15)} = 6.381$, $p = 0.027$; genotype×treatment: $F_{(1, 15)} = 3.069$, $p = 0.105$). These results suggested that OXA treatment might increase Aβ deposition in the brain in 3xTg-AD mice by increasing Aβ production via greater BACE1 expression and decreasing Aβ clearance via reduced NEP expression.

3.6. OXA increased tau hyperphosphorylation in the hippocampus in 3xTg-AD mice

NFTs formed by abnormally phosphorylated tau protein are another typical pathological characteristic in the AD brain and are positively correlated with the degree of dementia in AD patients (Liang et al., 2022). In the present study, phosphorylated tau (p-tau) protein in the hippocampus was observed by immunohistochemistry and western blotting (Fig. 7). The percentage of the p-tau immunopositive area in the hippocampus was significantly higher in the 3xTg-AD+Vehicle group than in the WT + Vehicle group (Fig. 7A and B, $p < 0.001$), and OXA treatment further increased the p-tau immunopositive area in the hippocampus in 3xTg-AD mice ($p < 0.001$) (two-way ANOVA: genotype: $F_{(1, 20)} = 298.650$, $p < 0.001$; treatment: $F_{(1, 20)} = 53.821$, $p < 0.001$; genotype×treatment: $F_{(1, 20)} = 33.347$, $p < 0.001$).

The expression levels of p-tau protein and total tau (t-tau) protein in the hippocampus in the mouse groups are shown in Fig. 7C–F. The expression levels of pT231 ($p = 0.001$) and AT8 ($p = 0.006$) in the hippocampus were significantly higher in the 3xTg-AD+Vehicle group than in the WT + Vehicle group, and OXA treatment further increased the expression levels of pT231 ($p = 0.005$) and AT8 ($p = 0.043$) in the hippocampus in 3xTg-AD mice (two-way ANOVA: pT231: genotype: $F_{(1, 15)} = 63.577$, $p < 0.001$; treatment: $F_{(1, 15)} = 9.172$, $p = 0.010$; genotype×treatment: $F_{(1, 15)} = 3.162$, $p = 0.101$; AT8: genotype: $F_{(1, 15)} = 29.224$, $p < 0.001$; treatment: $F_{(1, 15)} = 6.400$, $p = 0.026$; genotype×treatment: $F_{(1, 15)} = 0.460$, $p = 0.510$). In addition, the expression level of Tau5, which reflects the total amount of tau protein in the hippocampus, was significantly higher in the 3xTg-AD+Vehicle group than in the WT + Vehicle group ($p < 0.001$), and OXA treatment further increased the level of t-tau in the hippocampus in 3xTg-AD mice ($p < 0.001$) (two-way ANOVA: genotype: $F_{(1, 15)} = 179.259$, $p < 0.001$; treatment: $F_{(1, 15)} = 49.476$, $p < 0.001$; genotype×treatment: $F_{(1, 15)} = 28.868$, $p < 0.001$).

3.7. OXA aggravated the disturbance of the circadian locomotor rhythm in 3xTg-AD mice

Wheel-running activity was monitored to assess the behavioral circadian rhythm of the mice. In the 12 hour:12 hour light-dark (LD) environment, the mean robustness ($p = 0.023$, Fig. 8B), mean amplitude ($p = 0.002$, Fig. 8C) and interdaily stability (IS) ($p = 0.008$, Fig. 8D) were significantly lower in the 3xTg-AD + Vehicle group than in the WT + Vehicle group, but the intradaily variability (IV) was significantly higher in the 3xTg-AD+Vehicle group ($p = 0.011$, Fig. 8E). OXA treatment further decreased the robustness ($p = 0.038$), amplitude ($p = 0.048$) and IS ($p = 0.031$) in the 3xTg-AD+OXA group, while IV increased ($p = 0.016$) (two-way ANOVA: robustness: genotype: $F_{(1, 15)} = 17.490$, $p = 0.001$; treatment: $F_{(1, 15)} = 7.856$, $p = 0.016$; genotype×treatment: $F_{(1, 15)} = 0.235$, $p = 0.636$; amplitude: genotype: $F_{(1, 15)} = 41.943$, $p < 0.001$; treatment: $F_{(1, 15)} = 4.860$, $p = 0.048$; genotype×treatment: $F_{(1, 15)} = 0.825$, $p = 0.382$; IS: genotype: $F_{(1, 15)} = 43.823$, $p < 0.001$; treatment: $F_{(1, 15)} = 1.887$,

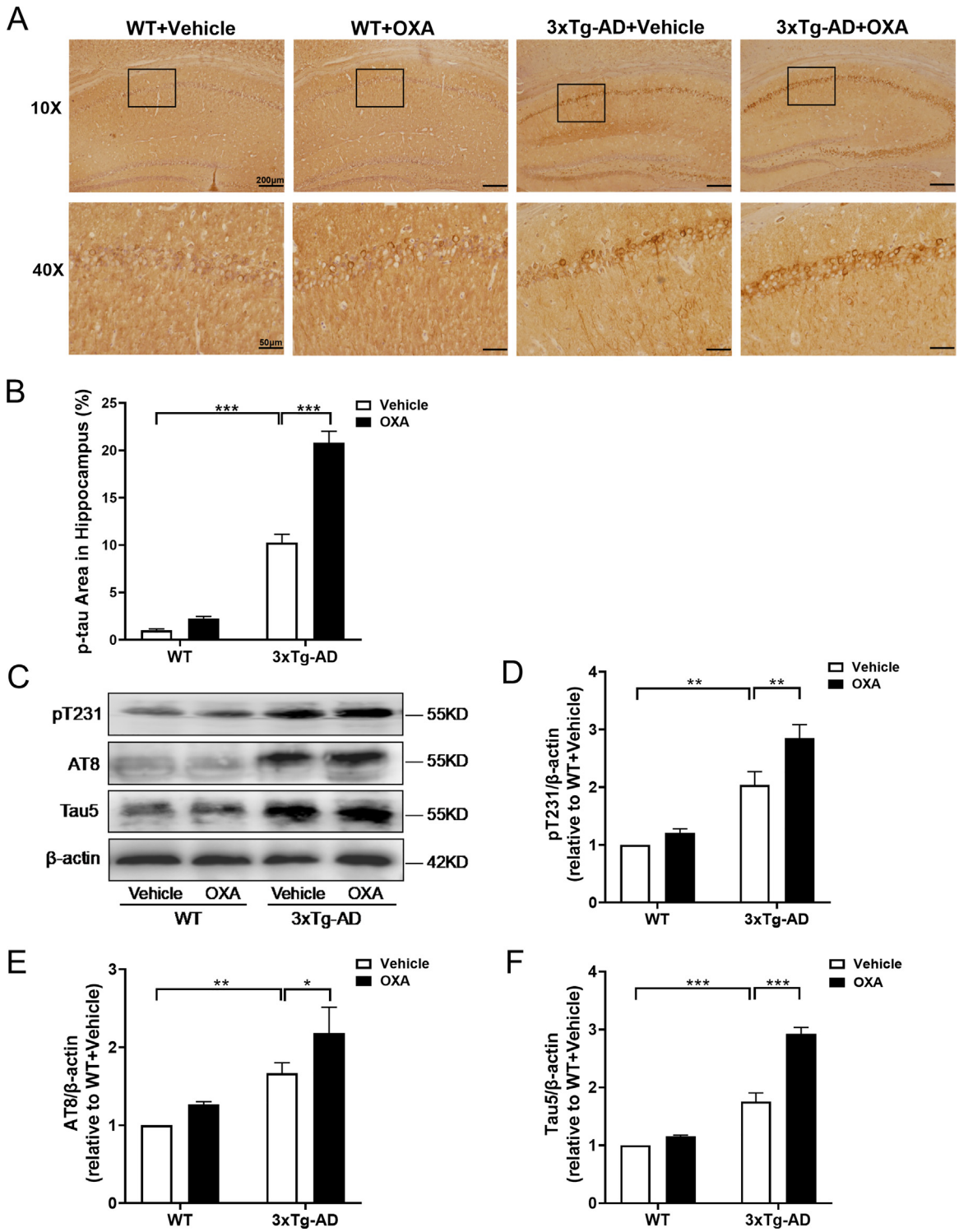

Fig. 7. OXA increased the abnormal phosphorylation levels of tau protein in the hippocampus in 3xTg-AD mice. (A) Representative images of immunohistochemical staining of phosphorylated tau protein in frozen sections of the hippocampus. (B) Bar plots showing the percentage of phosphorylated tau protein immunopositive area in the hippocampus (n = 5–6, $^{***}p < 0.001$). (C) Representative original immunoblots of pT231, AT8 and Tau5 in the hippocampus. (D-F) Bar plots showing the expression levels of pT231, AT8 and Tau5 in the hippocampus (n = 4, $^{*}p < 0.05$, $^{**}p < 0.01$, $^{***}p < 0.001$).

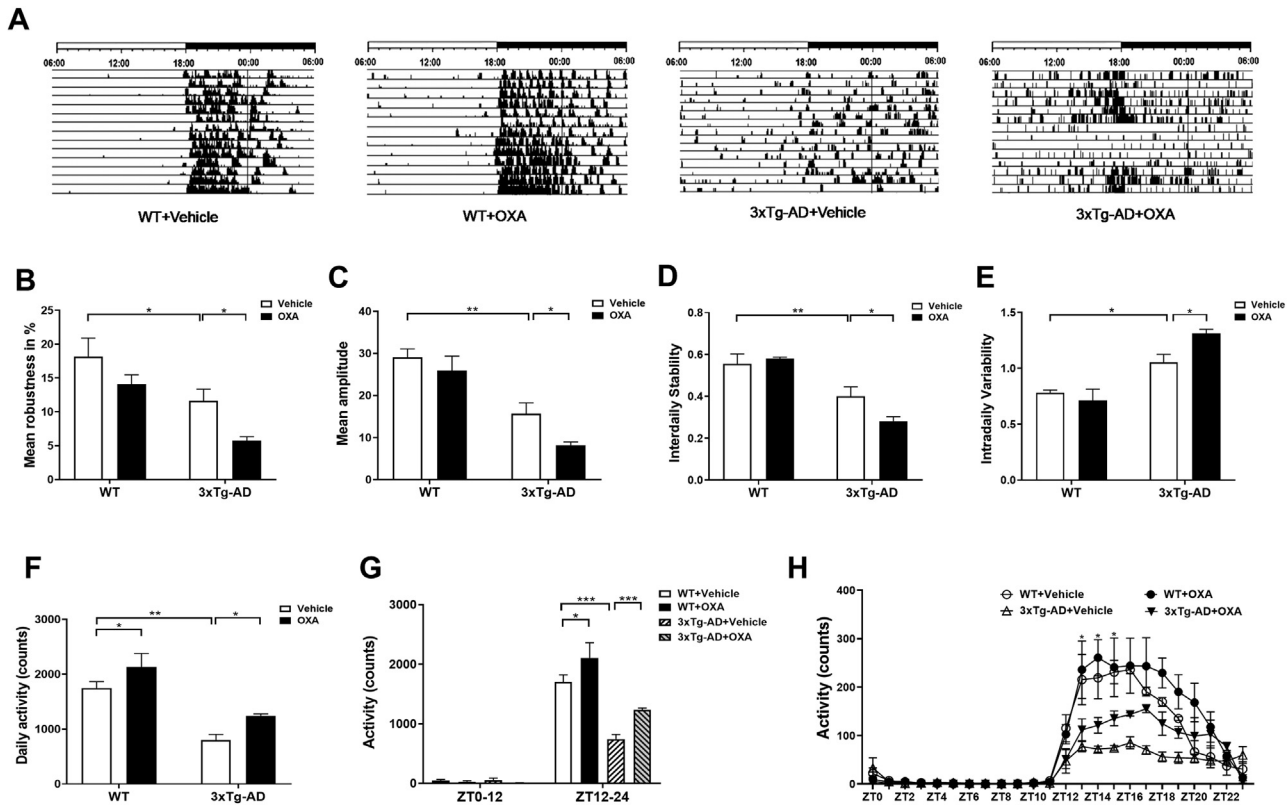

Fig. 8. OXA aggravated the disturbance of the circadian locomotor rhythm in 3xTg-AD mice. (A) Representative original wheel-running actograms of mice in the 4 groups entrained to the 12 hour:12 hour light-dark (LD) cycle. (B–E) Bar plots showing the mean robustness, mean amplitude, IS and IV of each group of mice. (F) Bar plots showing the total daily activity of the 4 mouse groups. (G) Bar plots showing the locomotor activity of the mice during ZT0-ZT12 (resting phase) and ZT12-ZT24 (active phase). (H) Line charts showing the average activity of the 4 groups of mice in each hour (n = 4, $^{*}p < 0.05$, $^{**}p < 0.01$, $^{***}p < 0.001$).

$p = 0.195$; genotype×treatment: $F_{(1, 15)} = 4.336$, $p = 0.059$; IV: genotype: $F_{(1, 15)}$=45.420, P<0.001; treatment: $F_{(1, 15)} = 2.079$, $p = 0.175$; genotype×treatment: $F_{(1, 15)} = 6.300$, $p = 0.027$). These results demonstrated that the circadian locomotor rhythm in the LD environment was disrupted in 3xTg-AD mice and that OXA treatment aggravated this disturbance.

In addition, the average daily activity ($p = 0.001$, Fig. 8F) and the activity in ZT12-ZT24 (active phase) ($p < 0.001$, Fig. 8G), especially in ZT13 ($p = 0.042$, Fig. 8H), ZT14 ($p = 0.023$) and ZT15 ($p = 0.037$), were significantly lower in the 3xTg-AD+Vehicle group than in the WT+Vehicle group, while daily activity ($p = 0.040$) and activity in ZT12-ZT24 ($p < 0.001$) were significantly higher in the 3xTg-AD+OXA group than in the 3xTg-AD+Vehicle group. In addition, OXA treatment increased the daily activity ($p = 0.043$) and activity in ZT12-ZT24 ($p = 0.035$) of WT mice (two-way ANOVA: daily activity: genotype: $F_{(1, 15)} = 35.265$, $p < 0.001$; treatment: $F_{(1, 15)} = 10.400$, $p = 0.007$; genotype×treatment: $F_{(1, 15)} = 0.001$, $p = 0.976$; activity in ZT12-ZT24: genotype: $F_{(1, 15)} = 73.814$, $p < 0.001$; treatment: $F_{(1, 15)} = 36.878$, $p < 0.001$; genotype×treatment: $F_{(1, 15)} = 7.393$, $p = 0.019$). These results indicated that OXA treatment increased the daily activity of both 3xTg-AD mice and WT mice, especially in the active phase.

4. Discussion

Dementia characterized by noticeable memory, language, thinking or behavioral symptoms is the main clinical feature of AD. Some clinical studies have found abnormal elevation of the level of OXA in the CSF in MCI and AD patients, accompanied by impaired cognitive function, reduced REM sleep and disrupted sleep-wake patterns (Gabelle et al., 2017; Heywood et al., 2018; Liguori et al., 2019; Liguori et al., 2016; Liguori et al., 2014). In APP/PS1 mice, which mainly exhibit Aβ deposition, chronic i.c.v. injection of OXA aggravates spatial learning and memory impairments (Li et al., 2020). However, the effects of OXA on other types of cognitive function in AD, such as working memory and recognition memory, are still unclear. Furthermore, considering the synergistic roles of Aβ and tau in AD pathogenesis (Busche and Hyman, 2020), it is important to clarify the effects of OXA in 3xTg-AD mice, which exhibit both Aβ plaques and tau phosphorylation. Intranasal administration allows OXA to be conveyed rapidly and directly to the central nervous system (Erichsen et al., 2021). Intranasal OXA administration results in substantial delivery throughout the brain in rhesus monkeys (Deadwyler et al., 2007), rats (Dhuria et al., 2009; Van de Bittner et al., 2018) and mice (Hanson et al., 2004); reduces wake-REM sleep transitions and REM sleep duration in narcolepsy patients with cataplexy (Baier et al., 2011; Weinhold et al., 2014); and triggers arousal in a rat model of cardiac arrest-induced coma (Modi et al., 2017). In addition, intranasal administration of OXA minimizes drug exposure in peripheral organs and tissues, thereby reducing adverse systemic side effects. Given the effectiveness and advantages of intranasal administration, we chose this method to deliver OXA in the present study.

To evaluate the effects of OXA on the learning and memory abilities of 3xTg-AD mice, the NORT, YMT and MWMT were performed. The results showed that OXA administration significantly aggravated the impairments in short-term working memory and long-term spatial memory in 3xTg-AD mice. In addition, a negative DI in the NORT was observed in the 3xTg-AD+OXA group. Given the results of the other behavioral tests, this nega-

tive DI might be the result of impaired recognition memory, but the possibility of neophobia should be considered (Binder et al., 2015). Orexin knockout mice exhibit poor spatial recognition performance (Dang et al., 2018), and cellular activation of hypothalamic orexin neurons facilitates short-term spatial memory in mice (Aitta-Aho et al., 2016); in rats, i.c.v. injection of OXA impairs performance in the MWMT (Aou et al., 2003). Here, we found that OXA administration induced spatial learning and memory impairments in WT mice but did not affect the recognition memory and short-term working memory of WT mice, indicating that the potential mechanisms by which OXA affects different types of cognitive functions differ under physiological conditions and AD pathological conditions.

LTP is an important phenotypic form of synaptic plasticity and is closely related to the formation of learning and memory (Bliss and Collingridge, 1993). Oddo et al. reported in vitro LTP impairment in brain slices from 6-month-old 3xTg-AD mice (Oddo et al., 2003). We previously observed in vivo LTP depression and long-term depression (LTD) facilitation in 9-month-old 3xTg-AD mice (Yan et al., 2022). However, the effects of OXA on hippocampal synaptic plasticity in 3xTg-AD mice have not been assessed. In the present study, in vivo electrophysiological recording showed that OXA did not affect basal synaptic transmission or presynaptic neurotransmitter release in the hippocampus in either WT mice or 3xTg-AD mice. HFS successfully induced LTP in each group, and LTP depression was observed in 3xTg-AD mice. Notably, OXA treatment exacerbated the hippocampal LTP depression in 3xTg-AD mice and induced hippocampal LTP depression in WT mice. These results may explain why OXA administration aggravated the impairments in cognitive behaviors in 3xTg-AD mice and induced impairments in WT mice. A previous study found that OXA treatment impairs in vitro hippocampal LTP in rats without affecting presynaptic neurotransmitter release (Aou et al., 2003), and we recently showed that chronic sleep deprivation depresses in vivo hippocampal LTP in both APP/PS1 mice and WT mice (Wang et al., 2021). More importantly, the present study showed that OXA administration increased the daily activity of both 3xTg-AD mice and WT mice and aggravated the disturbance of the circadian locomotor rhythm in 3xTg-AD mice. Considering that a normal circadian rhythm and sleep are important for regulating structural plasticity and synaptic strength (Raven et al., 2018), OXA might impair hippocampal synaptic plasticity by disrupting the circadian rhythm and increasing wakefulness.

Aβ deposition is the dominant pathological manifestation of AD and can impair cognitive function and accelerate the development of AD (Katzmarski et al., 2020; Tolar et al., 2021). In Tg2576 mice, which mainly exhibit Aβ pathology, i.c.v. injection of OXA increases Aβ levels in the hippocampal interstitial fluid by inducing wakefulness (Kang et al., 2009). In APP/PS1-21 and APP/PS1 mice, the deletion of orexin significantly reduces Aβ plaques in the brains and increases sleep time, whereas restoring hypothalamic orexin expression increases wakefulness and Aβ plaques in the brain (Roh et al., 2014). Consistent with these previous studies, administration of OXA significantly increased Aβ plaque deposition in the hippocampus and cortex in 3xTg-AD mice in the present study. Furthermore, considering that soluble Aβ oligomers form earlier than Aβ plaques and exert neurotoxicity (Lee et al., 2017; Tolar et al., 2021), we also measured the level of soluble Aβ oligomers in the hippocampus in 3xTg-AD mice. We found that intranasal administration of OXA significantly increased the level of soluble Aβ oligomers, which might be an important reason for the Aβ plaque formation, synaptic plasticity impairment and cognitive dysfunction observed in 3xTg-AD mice treated with OXA. In addition, our assessment of circadian rhythm based on wheel-running activity showed that OXA treatment decreased the robustness, amplitude and IS but increased IV and daily activity, especially activity in ZT12-ZT24, in 3xTg-AD mice, indicating that OXA effectively aggravated the circadian rhythm disturbance and increased wakefulness in 3xTg-AD mice. These changes might be closely related to the development of Aβ pathology.

Although the results of the present study and previous studies consistently demonstrate that OXA treatment increases Aβ levels in the brain in different mouse models of AD, the underlying mechanism is unclear. OXA has been reported to affect the phagocytosis and degradation of exogenous Aβ in microglia (An et al., 2017) and decrease Aβ clearance by the brain glymphatic system by reducing nighttime sleep (Dauvilliers, 2021). However, the effect of OXA on Aβ production has not been examined. In the present study, the expression level of BACE1, the rate-limiting enzyme in Aβ production (Hampel et al., 2021), was measured. We found that OXA treatment increased the expression of BACE1 in the hippocampus in 3xTg-AD mice, suggesting that OXA elevates Aβ levels by increasing Aβ production. In addition, NEP plays an important role in Aβ degradation (Campos et al., 2020; Ullah et al., 2021). We showed here that the expression of NEP in the hippocampus in 3xTg-AD mice decreased significantly after OXA treatment, indicating that OXA also increases Aβ levels in the brain in 3xTg-AD mice by decreasing NEP expression. These results indicate that OXA administration affects the expression levels of enzymes related to Aβ production and degradation, but whether these effects are related to circadian rhythm disruption and increased wakefulness and the potential mechanisms need to be further investigated.

NFTs formed by abnormal tau phosphorylation are another typical pathological feature in the AD brain and are positively correlated with the degree of dementia in AD patients (Ju and Tam, 2022). According to the amyloid cascade hypothesis, Aβ plays pivotal roles in AD pathogenesis and can lead to hyperphosphorylation of tau protein and NFT formation (Long and Holtzman, 2019; Shin et al., 2019). At the same time, accumulation of hyperphosphorylated tau can directly induce synaptic toxicity and cognitive impairment (Ma et al., 2017). This study is the first to examine the effect of OXA treatment on tau pathology. Immunohistochemistry and western blotting revealed that OXA administration increased abnormal tau phosphorylation at epitopes Ser202, Thr205 and Thr231 in the hippocampus in 3xTg-AD mice, possibly by increasing Aβ or other unknown mechanisms.

5. Conclusion

In the present study, exogenous OXA aggravated the impairments of multiple cognitive behaviors in 3xTg-AD mice, which exhibit both plaque and NFT pathologies, by worsening the impairment in in vivo hippocampal synaptic plasticity. OXA exerted detrimental effects in this AD mouse model by aggravating circadian rhythm disturbance, increasing wakefulness and reducing sleep, increasing Aβ production and decreasing Aβ clearance, thereby increasing Aβ oligomers, Aβ plaques and abnormal tau phosphorylation.

Verification

1. All authors disclose: No actual or potential conflicts of interest.
2. All authors verify that the data contained in the manuscript being submitted have not been previously published, have not been submitted elsewhere and will not be submitted elsewhere while under consideration at *Neurobiology of Aging*.
3. All authors have reviewed the contents of the manuscript being submitted, approve of its contents and validate the accuracy of the data.

Disclosure statement

The authors report no conflicts of interest.

Acknowledgements

This work was supported by the Research Project supported by Shanxi Scholarship Council of China (2020-083 - WMN), National Natural Science Foundation of China (82271484 - WMN, 82171428 - CHY, 82170523 - CJM), Applied Basic Research Program of Shanxi Province of China (20210302123306 - WZJ), "A batch of four" Medical Innovation Program through Science and Technology of Shanxi Province (2021XM33 -CHY), Shanxi "1331" Project Quality and Efficiency Improvement Plan (1331KSC- CJM).

CRediT authorship contribution statement

Yi-Ying Li: Investigation, Formal analysis, Writing – original draft. **Kai-Yue Yu:** Investigation, Formal analysis, Writing – original draft. **Yu-Jia Cui:** Investigation. **Zhao-Jun Wang:** Formal analysis, Funding acquisition. **Hong-Yan Cai:** Methodology, Funding acquisition. **Ji-Min Cao:** Writing – review & editing, Supervision, Funding acquisition. **Mei-Na Wu:** Conceptualization, Writing – review & editing, Supervision, Project administration, Funding acquisition.

References

Alzheimer's disease facts and figures, 2022. Alzheimers Dement 18 (4), 700–789. doi:10.1002/alz.12638.

Aitta-Aho, T., Pappa, E., Burdakov, D., Apergis-Schoute, J., 2016. Cellular activation of hypothalamic hypocretin/orexin neurons facilitates short-term spatial memory in mice. Neurobiol. Learn. Mem. 136, 183–188. doi:10.1016/j.nlm.2016.10.005.

An, H., Cho, M.H., Kim, D.H., Chung, S., Yoon, S.Y., 2017. Orexin impairs the phagocytosis and degradation of amyloid-beta fibrils by microglial cells. J. Alzheimers Dis. 58 (1), 253–261. doi:10.3233/JAD-170108.

Aou, S., Li, X.L., Li, A.J., Oomura, Y., Shiraishi, T., Sasaki, K., Imamura, T., Wayner, M.J., 2003. Orexin-A (hypocretin-1) impairs Morris water maze performance and CA1-Schaffer collateral long-term potentiation in rats. Neuroscience 119 (4), 1221–1228. doi:10.1016/s0306-4522(02)00745-5.

Baier, P.C., Hallschmid, M., Seeck-Hirschner, M., Weinhold, S.L., Burkert, S., Diessner, N., Goder, R., Aldenhoff, J.B., Hinze-Selch, D., 2011. Effects of intranasal hypocretin-1 (orexin A) on sleep in narcolepsy with cataplexy. Sleep Med. 12 (10), 941–946. doi:10.1016/j.sleep.2011.06.015.

Binder, S., Dere, E., Zlomuzica, A., 2015. A critical appraisal of the what-where-when episodic-like memory test in rodents: Achievements, caveats and future directions. Prog. Neurobiol. 130, 71–85. doi:10.1016/j.pneurobio.2015.04.002.

Bliss, T.V., Collingridge, G.L., 1993. A synaptic model of memory: long-term potentiation in the hippocampus. Nature 361 (6407), 31–39. doi:10.1038/361031a0.

Busche, M.A., Hyman, B.T., 2020. Synergy between amyloid-beta and tau in Alzheimer's disease. Nat. Neurosci. 23 (10), 1183–1193. doi:10.1038/s41593-020-0687-6.

Cai, H.Y., Yang, D., Qiao, J., Yang, J.T., Wang, Z.J., Wu, M.N., Qi, J.S., Holscher, C., 2021. A GLP-1/GIP Dual Receptor Agonist DA4-JC effectively attenuates cognitive impairment and pathology in the APP/PS1/Tau model of Alzheimer's disease. J. Alzheimers Dis. 83 (2), 799–818. doi:10.3233/JAD-210256.

Campos, C.R., Kemble, A.M., Niewoehner, J., Freskgard, P.O., Urich, E., 2020. Brain shuttle neprilysin reduces central amyloid-beta levels. PLoS One 15 (3), e0229850. doi:10.1371/journal.pone.0229850.

Chen, X.Y., Chen, L., Du, Y.F., 2017. Orexin-A increases the firing activity of hippocampal CA1 neurons through orexin-1 receptors. J. Neurosci. Res. 95 (7), 1415–1426. doi:10.1002/jnr.23975.

Dang, R., Chen, Q., Song, J., He, C., Zhang, J., Xia, J., Hu, Z., 2018. Orexin knockout mice exhibit impaired spatial working memory. Neurosci. Lett. 668, 92–97. doi:10.1016/j.neulet.2018.01.013.

Dauvilliers, Y., 2021. Hypocretin/Orexin, sleep and Alzheimer's disease. Front. Neurol. Neurosci. 45, 139–149. doi:10.1159/000514967.

Deadwyler, S.A., Porrino, L., Siegel, J.M., Hampson, R.E., 2007. Systemic and nasal delivery of orexin-A (Hypocretin-1) reduces the effects of sleep deprivation on cognitive performance in nonhuman primates. J. Neurosci. 27 (52), 14239–14247. doi:10.1523/JNEUROSCI.3878-07.2007.

Dhuria, S.V., Hanson, L.R., Frey 2nd, W.H., 2009. Intranasal drug targeting of hypocretin-1 (orexin-A) to the central nervous system. J. Pharm. Sci. 98 (7), 2501–2515. doi:10.1002/jps.21604.

Diering, G.H., Huganir, R.L., 2018. The AMPA receptor code of synaptic plasticity. Neuron 100 (2), 314–329. doi:10.1016/j.neuron.2018.10.018.

Dionisio-Santos, D.A., Karaahmet, B., Belcher, E.K., Owlett, L.D., Trojanczyk, L.A., Olschowka, J.A., O'Banion, M.K., 2021. Evaluating effects of glatiramer acetate treatment on amyloid deposition and tau phosphorylation in the 3xTg mouse model of Alzheimer's disease. Front. Neurosci. 15, 758677. doi:10.3389/fnins.2021.758677.

Dringenberg, H.C., 2020. The history of long-term potentiation as a memory mechanism: controversies, confirmation, and some lessons to remember. Hippocampus 30 (9), 987–1012. doi:10.1002/hipo.23213.

Eissman, J.M., Dumitrescu, L., Mahoney, E.R., Smith, A.N., Mukherjee, S., Lee, M.L., Scollard, P., Choi, S.E., Bush, W.S., Engelman, C.D., Lu, Q., Fardo, D.W., Trittschuh, E.H., Mez, J., Kaczorowski, C.C., Hernandez Saucedo, H., Widaman, K.F., Buckley, R.F., Properzi, M.J., Mormino, E.C., Yang, H.S., Harrison, T.M., Hedden, T., Nho, K., Andrews, S.J., Tommet, D., Hadad, N., Sanders, R.E., Ruderfer, D.M., Gifford, K.A., Zhong, X., Raghavan, N.S., Vardarajan, B.N., Alzheimer's Disease Neuroimaging, I., Alzheimer's Disease Genetics, C., Team, A.S., Pericak-Vance, M.A., Farrer, L.A., Wang, L.S., Cruchaga, C., Schellenberg, G.D., Cox, N.J., Haines, J.L., Keene, C.D., Saykin, A.J., Larson, E.B., Sperling, R.A., Mayeux, R., Cuccaro, M.L., Bennett, D.A., Schneider, J.A., Crane, P.K., Jefferson, A.L., Hohman, T.J., 2022. Sex differences in the genetic architecture of cognitive resilience to Alzheimer's disease. Brain 145 (7), 2541–2554. doi:10.1093/brain/awac177.

Erichsen, J.M., Calva, C.B., Reagan, L.P., Fadel, J.R., 2021. Intranasal insulin and orexins to treat age-related cognitive decline. Physiol. Behav. 234, 113370. doi:10.1016/j.physbeh.2021.113370.

Fanet, H., Tournissac, M., Leclerc, M., Caron, V., Tremblay, C., Vancassel, S., Calon, F., 2021. Tetrahydrobiopterin improves recognition memory in the triple-transgenic mouse model of Alzheimer's disease, without altering amyloid-beta and tau pathologies. J. Alzheimers Dis. 79 (2), 709–727. doi:10.3233/JAD-200637.

Frisoni, G.B., Altomare, D., Thal, D.R., Ribaldi, F., van der Kant, R., Ossenkoppele, R., Blennow, K., Cummings, J., van Duijn, C., Nilsson, P.M., Dietrich, P.Y., Scheltens, P., Dubois, B., 2022. The probabilistic model of Alzheimer disease: the amyloid hypothesis revised. Nat. Rev. Neurosci. 23 (1), 53–66. doi:10.1038/s41583-021-00533-w.

Gabelle, A., Jaussent, I., Hirtz, C., Vialaret, J., Navucet, S., Grasselli, C., Robert, P., Lehmann, S., Dauvilliers, Y., 2017. Cerebrospinal fluid levels of orexin-A and histamine, and sleep profile within the Alzheimer process. Neurobiol. Aging 53, 59–66. doi:10.1016/j.neurobiolaging.2017.01.011.

Hampel, H., Vassar, R., De Strooper, B., Hardy, J., Willem, M., Singh, N., Zhou, J., Yan, R., Vanmechelen, E., De Vos, A., Nistico, R., Corbo, M., Imbimbo, B.P., Streffer, J., Voytyuk, I., Timmers, M., Tahami Monfared, A.A., Irizarry, M., Albala, B., Koyama, A., Watanabe, N., Kimura, T., Yarenis, L., Lista, S., Kramer, L., Vergallo, A., 2021. The beta-Secretase BACE1 in Alzheimer's Disease. Biol. Psychiatry 89 (8), 745–756. doi:10.1016/j.biopsych.2020.02.001.

Hanson, L., Martinez, P.M., Taheri, S., Kamsheh, L., Mignot, E., Frey 2nd, W., 2004. Intranasal administration of hypocretin 1 (orexin A) bypasses the blood-brain barrier and target the brain: A new strategy for the treatment of narcolepsy. Drug Deliv. Tech. 4, 1–10.

Heywood, W.E., Hallqvist, J., Heslegrave, A.J., Zetterberg, H., Fenoglio, C., Scarpini, E., Rohrer, J.D., Galimberti, D., Mills, K., 2018. CSF pro-orexin and amyloid-beta38 expression in Alzheimer's disease and frontotemporal dementia. Neurobiol. Aging 72, 171–176. doi:10.1016/j.neurobiolaging.2018.08.019.

Jacobson, L.H., Hoyer, D., de Lecea, L., 2022. Hypocretins (orexins): The ultimate translational neuropeptides. J. Intern. Med. 291 (5), 533–556. doi:10.1111/joim.13406.

Ju, Y., Tam, K.Y., 2022. Pathological mechanisms and therapeutic strategies for Alzheimer's disease. Neural. Regen. Res. 17 (3), 543–549. doi:10.4103/1673-5374.320970.

Kang, J.E., Lim, M.M., Bateman, R.J., Lee, J.J., Smyth, L.P., Cirrito, J.R., Fujiki, N., Nishino, S., Holtzman, D.M., 2009. Amyloid-beta dynamics are regulated by orexin and the sleep-wake cycle. Science 326 (5955), 1005–1007. doi:10.1126/science.1180962.

Katzmarski, N., Ziegler-Waldkirch, S., Scheffler, N., Witt, C., Abou-Ajram, C., Nuscher, B., Prinz, M., Haass, C., Meyer-Luehmann, M., 2020. Abeta oligomers trigger and accelerate Abeta seeding. Brain Pathol. 30 (1), 36–45. doi:10.1111/bpa.12734.

Kraeuter, A.K., Guest, P.C., Sarnyai, Z., 2019. The Y-Maze for assessment of spatial working and reference memory in mice. Methods Mol. Biol. 1916, 105–111. doi:10.1007/978-1-4939-8994-2_10.

Lee, S.J., Nam, E., Lee, H.J., Savelieff, M.G., Lim, M.H., 2017. Towards an understanding of amyloid-beta oligomers: characterization, toxicity mechanisms, and inhibitors. Chem. Soc. Rev. 46 (2), 310–323. doi:10.1039/c6cs00731g.

Li, M., Meng, Y., Chu, B., Shen, Y., Xue, X., Song, C., Liu, X., Ding, M., Cao, X., Wang, P., Xu, S., Bi, J., Xie, Z., 2020. Orexin-A exacerbates Alzheimer's disease by inducing mitochondrial impairment. Neurosci. Lett. 718, 134741. doi:10.1016/j.neulet.2020.134741.

Li, R., Singh, M., 2014. Sex differences in cognitive impairment and Alzheimer's disease. Front. Neuroendocrinol. 35 (3), 385–403. doi:10.1016/j.yfrne.2014.01.002.

Liang, S.Y., Wang, Z.T., Tan, L., Yu, J.T., 2022. Tau Toxicity in Neurodegeneration. Mol. Neurobiol. 59 (6), 3617–3634. doi:10.1007/s12035-022-02809-3.

Liguori, C., Chiaravalloti, A., Nuccetelli, M., Izzi, F., Sancesario, G., Cimini, A., Bernardini, S., Schillaci, O., Mercuri, N.B., Fabio, P., 2017. Hypothalamic dysfunction is related to sleep impairment and CSF biomarkers in Alzheimer's disease. J. Neurol. 264 (11), 2215–2223. doi:10.1007/s00415-017-8613-x.

Liguori, C., Mercuri, N.B., Nuccetelli, M., Izzi, F., Cordella, A., Bernardini, S., Placidi, F., 2019. Obstructive sleep apnea may induce orexinergic system and cerebral beta-

amyloid metabolism dysregulation: is it a further proof for Alzheimer's disease risk? Sleep Med. 56, 171–176. doi:10.1016/j.sleep.2019.01.003.

Liguori, C., Nuccetelli, M., Izzi, F., Sancesario, G., Romigi, A., Martorana, A., Amoroso, C., Bernardini, S., Marciani, M.G., Mercuri, N.B., Placidi, F., 2016. Rapid eye movement sleep disruption and sleep fragmentation are associated with increased orexin-A cerebrospinal-fluid levels in mild cognitive impairment due to Alzheimer's disease. Neurobiol. Aging 40, 120–126. doi:10.1016/j.neurobiolaging.2016.01.007.

Liguori, C., Romigi, A., Nuccetelli, M., Zannino, S., Sancesario, G., Martorana, A., Albanese, M., Mercuri, N.B., Izzi, F., Bernardini, S., Nitti, A., Sancesario, G.M., Sica, F., Marciani, M.G., Placidi, F., 2014. Orexinergic system dysregulation, sleep impairment, and cognitive decline in Alzheimer disease. JAMA Neurol. 71 (12), 1498–1505. doi:10.1001/jamaneurol.2014.2510.

Liu, D., Dan, Y., 2019. A motor theory of sleep-wake control: arousal-action circuit. Annu. Rev. Neurosci. 42, 27–46. doi:10.1146/annurev-neuro-080317-061813.

Long, J.M., Holtzman, D.M., 2019. Alzheimer disease: an update on pathobiology and treatment strategies. Cell 179 (2), 312–339. doi:10.1016/j.cell.2019.09.001.

Lu, G.L., Lee, C.H., Chiou, L.C., 2016. Orexin A induces bidirectional modulation of synaptic plasticity: Inhibiting long-term potentiation and preventing depotentiation. Neuropharmacology 107, 168–180. doi:10.1016/j.neuropharm.2016.03.005.

Ma, R.H., Zhang, Y., Hong, X.Y., Zhang, J.F., Wang, J.Z., Liu, G.P., 2017. Role of microtubule-associated protein tau phosphorylation in Alzheimer's disease. J. Huazhong Univ. Sci. Technol. Med. Sci. 37 (3), 307–312. doi:10.1007/s11596-017-1732-x.

Modi, H.R., Wang, Q., Gd, S., Sherman, D., Greenwald, E., Savonenko, A.V., Geocadin, R.G., Thakor, N.V., 2017. Intranasal post-cardiac arrest treatment with orexin-A facilitates arousal from coma and ameliorates neuroinflammation. PLoS One 12 (9), e0182707. doi:10.1371/journal.pone.0182707.

Oddo, S., Caccamo, A., Shepherd, J.D., Murphy, M.P., Golde, T.E., Kayed, R., Metherate, R., Mattson, M.P., Akbari, Y., LaFerla, F.M., 2003. Triple-transgenic model of Alzheimer's disease with plaques and tangles: intracellular Abeta and synaptic dysfunction. Neuron 39 (3), 409–421.

Raven, F., Van der Zee, E.A., Meerlo, P., Havekes, R., 2018. The role of sleep in regulating structural plasticity and synaptic strength: Implications for memory and cognitive function. Sleep Med. Rev. 39, 3–11. doi:10.1016/j.smrv.2017.05.002.

Reiss, A.B., Arain, H.A., Stecker, M.M., Siegart, N.M., Kasselman, L.J., 2018. Amyloid toxicity in Alzheimer's disease. Rev. Neurosci. 29 (6), 613–627. doi:10.1515/revneuro-2017-0063.

Roda, A.R., Serra-Mir, G., Montoliu-Gaya, L., Tiessler, L., Villegas, S., 2022. Amyloid-beta peptide and tau protein crosstalk in Alzheimer's disease. Neural. Regen. Res. 17 (8), 1666–1674. doi:10.4103/1673-5374.332127.

Roh, J.H., Jiang, H., Finn, M.B., Stewart, F.R., Mahan, T.E., Cirrito, J.R., Heda, A., Snider, B.J., Li, M., Yanagisawa, M., de Lecea, L., Holtzman, D.M., 2014. Potential role of orexin and sleep modulation in the pathogenesis of Alzheimer's disease. J. Exp. Med. 211 (13), 2487–2496. doi:10.1084/jem.20141788.

Sciaccaluga, M., Megaro, A., Bellomo, G., Ruffolo, G., Romoli, M., Palma, E., Costa, C., 2021. An unbalanced synaptic transmission: cause or consequence of the amyloid oligomers neurotoxicity? Int. J. Mol. Sci. 22 (11), 5991. doi:10.3390/ijms22115991.

Selbach, O., Bohla, C., Barbara, A., Doreulee, N., Eriksson, K.S., Sergeeva, O.A., Haas, H.L., 2010. Orexins/hypocretins control bistability of hippocampal long-term synaptic plasticity through co-activation of multiple kinases. Acta. Physiol. (Oxf) 198 (3), 277–285. doi:10.1111/j.1748-1716.2009.02021.x.

Serge, G., Pedro, R.-N., José, A.M., Claire, W., 2021. World Alzheimer Report 2021 Journey through the diagnosis of dementia.

Shin, W.S., Di, J., Cao, Q., Li, B., Seidler, P.M., Murray, K.A., Bitan, G., Jiang, L., 2019. Amyloid β-protein oligomers promote the uptake of tau fibril seeds potentiating intracellular tau aggregation. Alzheimers Res. Ther. 11 (1), 86. doi:10.1186/s13195-019-0541-9.

Tolar, M., Hey, J., Power, A., Abushakra, S., 2021. Neurotoxic soluble amyloid oligomers drive Alzheimer's pathogenesis and represent a clinically validated target for slowing disease progression. Int. J. Mol. Sci. 22 (12), 6355. doi:10.3390/ijms22126355.

Ullah, R., Park, T.J., Huang, X., Kim, M.O., 2021. Abnormal amyloid beta metabolism in systemic abnormalities and Alzheimer's pathology: Insights and therapeutic approaches from periphery. Ageing Res. Rev. 71, 101451. doi:10.1016/j.arr.2021.101451.

Van de Bittner, G.C., Van de Bittner, K.C., Wey, H.Y., Rowe, W., Dharanipragada, R., Ying, X., Hurst, W., Giovanni, A., Alving, K., Gupta, A., Hoekman, J., Hooker, J.M., 2018. Positron emission tomography assessment of the intranasal delivery route for Orexin A. ACS Chem. Neurosci. 9 (2), 358–368. doi:10.1021/acschemneuro.7b00357.

Wang, C., Gao, W.R., Yin, J., Wang, Z.J., Qi, J.S., Cai, H.Y., Wu, M.N., 2021. Chronic sleep deprivation exacerbates cognitive and synaptic plasticity impairments in APP/PS1 transgenic mice. Behav. Brain Res. 412, 113400. doi:10.1016/j.bbr.2021.113400.

Wang, C., Wang, Q., Ji, B., Pan, Y., Xu, C., Cheng, B., Bai, B., Chen, J., 2018. The Orexin/Receptor system: molecular mechanism and therapeutic potential for neurological diseases. Front. Mol. Neurosci. 11, 220. doi:10.3389/fnmol.2018.00220.

Weinhold, S.L., Seeck-Hirschner, M., Nowak, A., Hallschmid, M., Goder, R., Baier, P.C., 2014. The effect of intranasal orexin-A (hypocretin-1) on sleep, wakefulness and attention in narcolepsy with cataplexy. Behav. Brain Res. 262, 8–13. doi:10.1016/j.bbr.2013.12.045.

Wu, M., Zhou, F., Cao, X., Yang, J., Bai, Y., Yan, X., Cao, J., Qi, J., 2018. Abnormal circadian locomotor rhythms and Per gene expression in six-month-old triple transgenic mice model of Alzheimer's disease. Neurosci. Lett. 676, 13–18. doi:10.1016/j.neulet.2018.04.008.

Yan, X.D., Qu, X.S., Yin, J., Qiao, J., Zhang, J., Qi, J.S., Wu, M.N., 2022. Adiponectin ameliorates cognitive behaviors and in vivo synaptic plasticity impairments in 3xTg-AD Mice. J. Alzheimers Dis. 85 (1), 343–357. doi:10.3233/JAD-215063.

Yang, L., Zou, B., Xiong, X., Pascual, C., Xie, J., Malik, A., Xie, J., Sakurai, T., Xie, X.S., 2013. Hypocretin/orexin neurons contribute to hippocampus-dependent social memory and synaptic plasticity in mice. J. Neurosci. 33 (12), 5275–5284. doi:10.1523/JNEUROSCI.3200-12.2013.

Yue, F., Feng, S., Lu, C., Zhang, T., Tao, G., Liu, J., Yue, C., Jing, N., 2021. Synthetic amyloid-beta oligomers drive early pathological progression of Alzheimer's disease in nonhuman primates. iScience 24 (10), 103207. doi:10.1016/j.isci.2021.103207.

Zhang, Z., Wang, H.J., Wang, D.R., Qu, W.M., Huang, Z.L., 2017. Red light at intensities above 10 lx alters sleep-wake behavior in mice. Light Sci. Appl. 6 (5), e16231. doi:10.1038/lsa.2016.231.

Zhou, F., Yan, X.D., Wang, C., He, Y.X., Li, Y.Y., Zhang, J., Wang, Z.J., Cai, H.Y., Qi, J.S., Wu, M.N., 2020. Suvorexant ameliorates cognitive impairments and pathology in APP/PS1 transgenic mice. Neurobiol. Aging 91, 66–75. doi:10.1016/j.neurobiolaging.2020.02.020.